

Magnetic and structural study of electric double-layered ferrofluid with $\text{MnFe}_2\text{O}_4@ \gamma\text{-Fe}_2\text{O}_3$ nanoparticles of different mean diameters: Determination of the magnetic correlation distance

E. S. Gonçalves,* D. R. Cornejo, C. L. P. Oliveira, and A. M. Figueiredo Neto
Instituto de Física, Universidade de São Paulo, São Paulo, Brazil

J. Depeyrot
Instituto de Física, Universidade de Brasília, Brasília, Brazil

F. A. Tourinho
Instituto de Química, Universidade de Brasília, Brasília, Brazil

R. Aquino
Faculdade UnB Planaltina, Universidade de Brasília, Brasília, Brazil

(Received 13 February 2015; published 30 April 2015)

Magnetic fluids based on manganese ferrite nanoparticles were studied from the structural point of view through small angle x-rays scattering (SAXS) and from the magnetic point of view through zero-field cooling and field cooling (ZFC-FC) and ac susceptibility measurements (MS). Three different colloids with particles mean diameters of 2.78, 3.42, and 6.15 nm were investigated. The size distribution obtained from SAXS measurements follows a log-normal behavior. The ZFC-FC and MS results revealed the presence of an important magnetic interaction between the nanoparticles, characterized by a magnetic correlation distance Λ . The colloidal medium can be pictures as composed by magnetic cluster constituted by N interacting particles. These magnetic clusters are not characterized by a physical aggregation of particles. The energy barrier energy obtained is consistent with the existence of this magnetic clusters. Besides the magnetic interaction between particles, confinement effects must be included to account for the experimental values of the magnetic energy barrier encountered.

DOI: [10.1103/PhysRevE.91.042317](https://doi.org/10.1103/PhysRevE.91.042317)

PACS number(s): 83.80.Hj, 75.75.-c, 75.50.Mm, 61.05.cf

I. INTRODUCTION

The study of magnetic properties of granular materials is an interesting subject of research in the field of condensed matter physics [1,2]. Due to their technological applications, in particular in information-storage devices, much effort has been devoted to understanding the magnetic behavior of these systems under the action of external magnetic fields. In the case of this type of device, grains are embedded in a solid nonmagnetic matrix and only the grains' magnetic moments respond to the external field, since they do not rotate or diffuse in the matrix. Different characteristics of the granular medium are responsible for their magnetic properties, e.g., the size distribution of grains, their shape, typical dimension, magnetic moment, and magnetic anisotropy.

On the other hand, magnetic nanofluids or ferrofluids, are colloidal dispersions of magnetic nanoparticles in a liquid carrier [3,4]. The great interest in investigating the magnetic properties of ferrofluids is due not only to their fundamental aspects but also to their technological applications, e.g., heat transfer [5] or sealing [6], as well as biological applications, including cancer treatment by magnetic hyperthermia [7], drug delivery [8], and contrast for magnetic resonance imaging (MRI) [9]. In the case of magnetic fluids, particles are free to rotate in the liquid medium, and different physical processes may occur as a function of the external magnetic field. The magnetic moment of the particle may align parallel to the external field, without the physical rotation of the particle

(Néel rotation), or the particle rotates itself to align the magnetic moment parallel to the field (Brownian rotation) [10]. The different response time depends on parameters of the particle, e.g., volume, magnetocrystalline anisotropy, and of the fluid carrier, e.g., its viscosity. Among the experimental techniques used to investigate the magnetic properties of granular materials, the analysis of the magnetization under conditions of zero-field cooling (ZFC) and field cooling (FC) is widely used, as well as the ac magnetic susceptibility (MS) of the system [11–13]. The ZFC-FC technique allows us to determine the average blocking temperature (T_B) of the system, while the MS allows us to reveal the behavior of that parameter under time-dependent fields. Interestingly, from the magnetization measurements and appropriate modeling, it is possible to extract the blocking temperature distribution, which reveals the particles' size-distribution function [1]. Nanostructured magnetic materials are often studied whether to determine the complex ac susceptibility [14] or the field dependence of the blocking temperature [15], and the coercive field [16] as a function of temperature and changes in the anisotropy constant [17,18] were investigated as well. Interactions between nanoparticles were investigated [1,17,19,20] also by calculations of dipole-dipole-coupled nanoparticles' relaxation times [21] and through mean-field theory [22].

The analysis of the ZFC-FC magnetization curves is highly improved if a complementary experimental technique is employed. Among these techniques, small-angle x-ray scattering (SAXS) is one of the most adequate. The advantage of SAXS is that one can obtain directly from the scattering intensity curve the size-distribution function of particles in ferrofluids, and also evaluates the presence of clusters [23,24].

*eduardos@if.usp.br

From the magnetic measurements we are able to measure the extent of the magnetic coupling between particles and correlate it with the structural information provided by SAXS, even if these particles are not grouped in clusters that impose fluctuations in the electronic density function of the medium. This aspect is particularly interesting in the physics of magnetic colloids. Different correlation lengths exist, related to the ordering of the particles. Particles may agglomerate in physical clusters (dimers, trimers, etc.), characterized by a positional correlation length and strong electronic density spatial fluctuations. On the other hand, even in the absence of physical clusters, the magnetic moments of the particles introduce an additional correlation length, which informs how the system respond to external magnetic fields, as isolated particles or collectively (in a particular length scale, Λ , named magnetic correlation distance). The magnetic correlation volume Λ^3 may be considered as a “magnetic cluster.”

In this work we investigate the blocking temperature T_B , the magnetic susceptibility χ , the magnetic anisotropy energy density K , and the size distribution function of magnetic colloidal dispersions of $\text{MnFe}_2\text{O}_4@ \gamma\text{-Fe}_2\text{O}_3$ core-shell ferrite nanoparticles of different particles’ mean diameters. The techniques employed are the ZFC-FC and SAXS. The existence of physical and magnetic clusters is also investigated. The paper is organized as follows: in Sec. II the theoretical background is presented; Sec. III describes the materials and experimental methods; Sec. IV includes the results and discussion, followed by conclusions.

II. THEORETICAL BACKGROUND

Since the nanoparticles in a ferrofluid are sufficiently small (typical size 10 nm) they have a single magnetic domain [25]. Usually, at room temperature, ferrofluids are superparamagnetic so the thermal energy is large enough for the magnetic moment to overcome the anisotropy energy barrier and flip between two equivalent directions along the easy axis. The characteristic time of this process is described by the Néel-Arrhenius equation [26]:

$$\tau_N = \tau_0 \exp\left(\frac{E_a}{k_B T}\right), \quad (1)$$

where k_B is the Boltzmann constant, T is the absolute temperature, τ_0 is the characteristic time, usually in the range $10^{-9} \text{ s} \sim 10^{-12} \text{ s}$, and $E_a = KV$ corresponds to the anisotropic energy barrier, K is the magnetic anisotropy energy density, and V the volume of the monodomain particle in the absence of magnetic field. On the other hand, if the thermal energy is not enough for the magnetic moment to overcome the energy barrier between these two equivalent directions, the particle is in the blocked state.

The temperature at which the system transits from blocked to superparamagnetic state is the blocking temperature T_B , which depends on the characteristic time τ_m of the experiment performed to determine T_B . In a system composed by monodisperse particles of volume V_0 , the blocking temperature is defined by

$$T_B = \frac{K V_0}{k_B \log\left(\frac{\tau_m}{\tau_0}\right)}. \quad (2)$$

A common way to determine T_B is keep τ_m constant and change the system temperature. In the zero-field cooling and field cooling protocol the sample is quickly frozen in the absence of magnetic field, preserving the random orientation of nanoparticle’s easy axis. In the following, a small magnetic field ($H = 50 \text{ Oe}$) is applied to the sample and the temperature is raised until a maximum value. After that, the sample temperature is slowly decreased in the presence of the magnetic field. For a system consisting of uniaxial, single domain, and noninteracting particles, the initial susceptibility of a particle of volume V at temperature T is given by Eqs. (3) for particles in the superparamagnetic (χ_{SP}) and in the blocked (χ_{BL}) states [27,28]:

$$\begin{aligned} \chi_{\text{SP}} &= \frac{M_s^2 V}{3k_B T}, \quad T > T_B, \\ \chi_{\text{BL}} &= \frac{M_s^2}{3K}, \quad T < T_B, \end{aligned} \quad (3)$$

where M_s is the saturation magnetization of the nanoparticle at $T = 0 \text{ K}$.

In a system composed of noninteracting polydisperse particles, which volumes follows a distribution $f(V)$, the susceptibility of the zero-field cooling curve is described by Eq. (4), while the susceptibility of the field cooling process is written in Eq. (5) [12,29] using the reduced variables $t_B = T_B / \langle T_B \rangle = V / \langle V \rangle$ and $t = T / \langle T_B \rangle$. The first term in both equations is the contribution of particles already in the superparamagnetic state, while the second term refers to particles in the blocked state:

$$\chi_{\text{ZFC}} = \frac{M_s^2}{3K} \left[\log\left(\frac{\tau_m}{\tau_0}\right) \frac{1}{t} \int_0^t t_B f(t_B) dt_B + \int_t^\infty f(t_B) dt_B \right] \quad (4)$$

$$\chi_{\text{FC}} = \frac{M_s^2}{3K} \log\left(\frac{\tau_m}{\tau_0}\right) \left[\frac{1}{t} \int_0^t t_B f(t_B) dt_B + \int_t^\infty f(t_B) dt_B \right]. \quad (5)$$

The magnetic susceptibility χ of a system subjected to an ac field is complex ($\chi = \chi' + i\chi''$). The imaginary part is related to dissipation losses [14,30], and its maximum value is achieved when $T = T_B$. As the blocking temperature depends on the measurement time, χ'' peak depends on the field’s frequency.

III. MATERIALS AND METHODS

Magnetic colloids based on manganese ferrite nanoparticles dispersed in aqueous acid medium were synthesized at Universidade de Brasília, Brazil (UnB) by using a well-proven procedure developed in three steps [31,32]. First, MnFe_2O_4 nanoparticles are obtained by hydrothermal coprecipitation of aqueous solutions of metal mixtures in an alkaline medium under vigorous stirring. Mean particle size is controlled here during the ferrofluid elaboration by the hydroxide concentration [33]. Then, the precipitate is washed in water and treated with a HNO_3 solution to reduce the ion excess and clean the particle surface. To protect the particle against acid dissolution, the precipitate has to be thermally treated with a

TABLE I. Mean diameter $\langle d \rangle$ of the nanoparticles determined by small angle x-rays scattering and distribution width of the log-normal function of the volume (σ_V) and blocking temperature (σ_T) of the particles, numerical concentration of particles (c), and magnetic correlation distance (Λ).

Sample	$\langle d \rangle$ (nm)	σ_V	σ_T	c (10^{17}cm^{-3})	Λ (nm)
Mn3	2.78 ± 0.12	1.56	0.45	9	25.1
Mn4	3.42 ± 0.12	1.44	0.55	5	24.0
Mn6	6.15 ± 0.09	1.55	0.66	1	39.4

ferric nitrate solution, which creates a maghemite surface layer onto the particles core. Finally, these core-shell nanoparticles are peptized in water at $\text{pH} \sim 3$, i.e., at an ionic strength around $10^{-3} \text{mol L}^{-1}$ leading to long-term stable colloidal dispersions. In order to describe the chemical composition heterogeneity of such nanoparticles, we use a core-shell model well supported by chemical titrations and x-ray diffraction measurements [32], which gives the particle volume fraction, the volume fraction of the maghemite shell and its corresponding thickness. Three different colloids with mean particles diameter $\langle d \rangle$ given in Table I were investigated. The particles' volume concentration was fixed $\phi = 1\%$. Particles' concentrations [$c \sim 0.06/(\pi \langle d \rangle^3)$] were also evaluated.

A commercial Quantum Design MPMS SQUID (Superconducting Quantum Interference Device) was used to measure the magnetic properties of ferrofluids, performing the zero-field cooling and field cooling protocol (temperature range from 5 to 250 K) and the susceptibility $\chi(T)$ to ac magnetic field (frequency range from 0.21 to 710 Hz). All samples were confined in small glass tubes sealed with UV-sensitive resin.

Small angle x-rays scattering measurements were made on a laboratory based SAXS instrument Bruker AXS NanoStar placed at the Institute of Physics of University of São Paulo, Brazil. This equipment is improved by the use of microfocus source Genix3D coupled with Fox3D multilayer optics and two sets of scatterless slits for beam definition, all provided by Xenocs. The wavelength of the incoming monochromatic x-ray beam was $\lambda = 0.154 \text{nm}$ ($\text{Cu } K\alpha$) and the sample to detector distance was 1.03 m, providing a scattering vector \vec{q} , whose modulus lies in the interval from 0.05nm^{-1} to 2.5nm^{-1} , $q = 4\pi(\sin \theta)/\lambda$ and 2θ the scattering angle. The 2D scattering data was collected on a Vantec2000 detector and the integration of the SAXS patterns were performed by the use of the Bruker SAXS software. Samples were encapsulated in Lindemann glass capillaries, with diameter $\phi_c = 1.5 \text{mm}$. The scattering data were obtained by 5400 s of exposition and the data treatment was performed with the program GIFT [24].

IV. RESULTS AND DISCUSSION

A. Size distribution function (SAXS)

Small angle x-rays scattering curves (scattering intensity I_s as a function of the modulus of the scattering vector q) were obtained for each sample, and are shown in Figs. 1(a)–1(c). These results were analyzed following Glatter's method [23,24], using the GIFT software. In this framework, theoretical

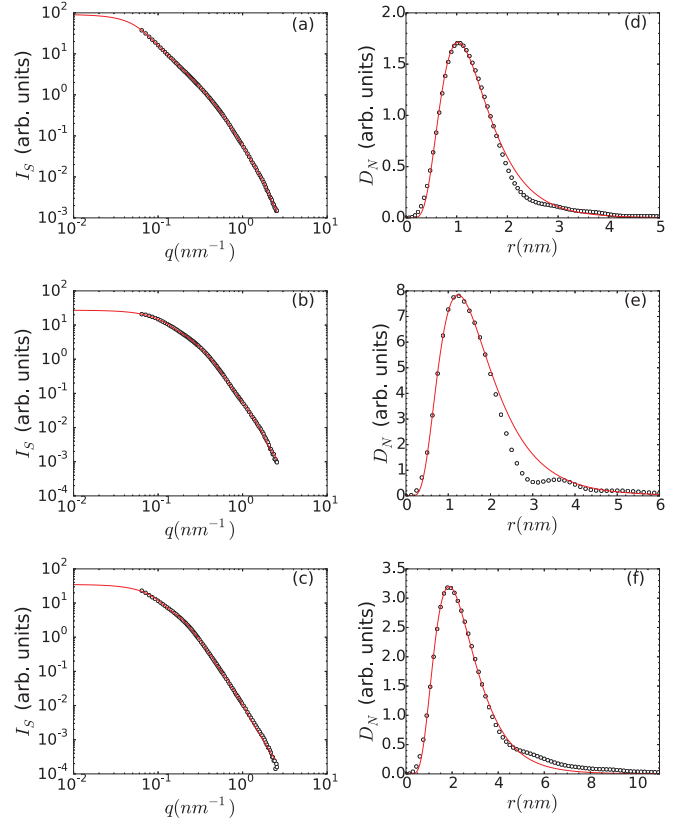


FIG. 1. (Color online) X-ray scattering intensity as a function of the modulus of the scattering vector. (a) Mn3, (b) Mn4, (c) Mn6. Particle's radius numerical distribution function. (d) Mn3, (e) Mn4, (f) Mn6. Open circles represent experimental data and continuous line the best fit of correspondent function.

scattering intensity I_s^G is written as

$$I_s^G(q) = \text{constant} \times \int D_N(r)[V(r)]^2 I_{\text{sp}}(q,r) dr, \quad (6)$$

where the scatterers are assumed to be a collection of polydisperse noninteracting spheres of radius r , volume V , normalized radius distribution function (in terms of the number of particles) $D_N(r)$, and I_{sp} the normalized scattering intensity due to a sphere of radius r . This procedure allows us to determine the size distribution function $D_N(r)$ from the fit of the experimental scattering curves to $I_s^G(q)$. The continuous lines in Figs. 1(a)–1(c) are the best fit of Eq. (6) to the experimental data. From these fits the size distribution functions were obtained and are shown in Figs. 1(d)–1(f), together with log-normal functions fitted to those data. In all the cases there is a small deviation from the log-normal dependence of D_N with r in the range of large particles.

The mean particle's diameter $\langle d \rangle$ was calculated as

$$\langle d \rangle = 2 \int r D_N(r) dr,$$

and the results are presented in Table I.

The bumps observed in Figs. 1(d)–1(f) indicate that bigger scatterers exist in the system. From the area below the main peak and that below the bumps we can evaluate the numerical percentage of these scatterers with respect to the amount of

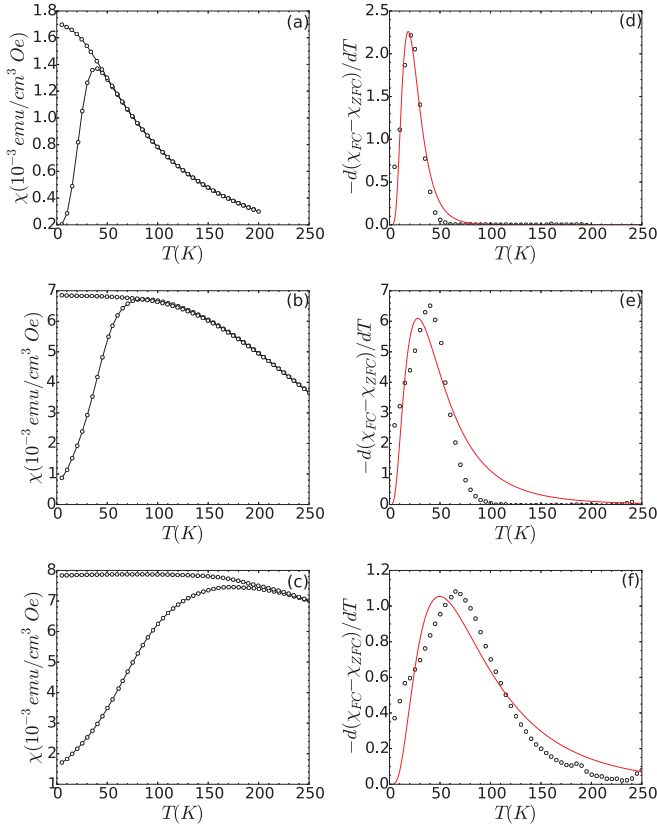


FIG. 2. (Color online) ZFC-FC magnetization curves. Magnetic susceptibilities in the condition of field cooling (higher values) and zero-field cooling (lower values): (a) Mn3, (b) Mn4, and (c) Mn6. Blocking temperature distribution function. Open circles represent the experimental data obtained from the derivative $d(\chi_{FC} - \chi_{ZFC})/dT$, where χ_{FC} and χ_{ZFC} represent the susceptibilities in the condition of field cooling and zero-field cooling, respectively. continuous line represents the best log-normal fit: (d) Mn3, (e) Mn4, (f) Mn6.

isolated particles. These values are about 5%, 6%, and 10% for the ferrofluids Mn3, Mn4, and Mn6, respectively. Our experimental results ($q > 5 \times 10^{-2} \text{ nm}^{-1}$) do not permit us to obtain more details about the shape and shape anisotropy of these larger scatterers (could be large single particles or small physical clusters, like dimmers or trimmers). They are present, but their amount is small. In summary, the SAXS results indicate that the system may be considered as composed (mainly) by isolated particles of mean diameter $\langle d \rangle$, without the presence of large amount of physical clusters.

B. Magnetic properties

Figures 2(a)–2(c) shows the ZFC-FC magnetization data of the $\text{MnFe}_2\text{O}_4 @ \gamma\text{-Fe}_2\text{O}_3$ ferrofluid samples Mn3, Mn4, and Mn6. The maximum of the ZFC curves shifts to higher temperatures as the mean diameter of the particles increases. These results indicate that the mean blocking temperature of the nanoparticles increases as $\langle d \rangle$ increases. Another remark about the data shown in those figures is that the maximum of the ZFC curve in the three cases is located near the temperature in which the ZFC and the FC curves split. In the framework of the model of noninteracting particles [29] it means that

the blocking temperature distribution $f(T_B)$ is expected to be narrow.

Following the Stoner-Wohlfarth (SW) model [34], suitable for describing uniaxial, single-domain, and noninteracting particles, the blocking temperature distribution can be obtained by Eq. (7):

$$f(T_B) \propto -\frac{d(\chi_{FC} - \chi_{ZFC})}{dT}, \quad (7)$$

where χ_{FC} and χ_{ZFC} represent the dc magnetic susceptibilities at FC and ZFC, respectively. According to the SW model, the relationship between the energy barrier and the blocking temperature (at zero applied field) is given by the linear Eq. (2). This implies that both size particles and blocking temperature function distributions must be proportional to each other.

The functions $f(T_B)$ obtained with the three ferrofluid samples are shown in Figs. 2(d)–2(f). Log-normal functions were fitted to these results and are also plotted in Figs. 2(d)–2(f). The difference between the log-normal curves and the experimental $f(T_B)$ increases as the particle's mean diameter increases. This result, commonly observed in granular systems, can be due to magnetic dipolar interaction between nanoparticles [1].

To test this hypothesis, the blocking temperature distribution experimental curves were compared with the volume distribution ones obtained with the SAXS analysis, checking the validity of the SW model in our systems. Let us compare the width of the distribution functions of Figs. 1(d)–1(f) and 2(d)–2(f). The log-normal dimensionless parameter σ_i ($i = T, V$), obtained through the fitting of the experimental data, was used to study the size and blocking temperature distribution function broadness. The narrower distributions obtained in the magnetic measurements with respect to those from the SAXS experiments in all the cases investigated here (see Table I) is an indication of the existence of interactions between nanoparticles, mainly from dipolar origin [1]. In this scenario, the model of noninteracting particles seems to be not fully adapted to the present case. The dipolar interactions leads to a coupling between particles over a magnetic correlation distance Λ [35], which affects the distribution width of the $f(T_B)$ curves.

The number of interacting particles (N) inside the correlation volume Λ^3 can be estimated from the distribution widths of the particle's volume (SAXS) and blocking temperature (magnetic measurements) as

$$N = \left(\frac{\sigma_V}{\sigma_T} \right)^2, \quad (8)$$

$$\Lambda^3 = \frac{N V_m}{\phi}, \quad (9)$$

where ϕ is the particles' volume concentration and $V_m = (\pi/6)\langle d \rangle^3$ the volume of the mean particle. N decreases as the mean diameter of particles increases, as shown in Table II. Our results indicate that in the colloid with the smallest particles (Mn3) the interparticle magnetic correlation extends to distances that involve the largest number of particles, with respect to the colloids with bigger particles. Values of the magnetic correlation volumes for the three samples are also shown in Table II. While the smaller particles' samples present

TABLE II. Magnetic properties of ferrofluids: Number of interacting particles N in the correlation volume Λ^3 , cluster's energy barrier experimentally determined ($E_a K_B^{-1}$) and theoretical prediction ($K_{\text{bulk}} V_m \sqrt{N} K_B^{-1}$), and surface anisotropy constant K_s .

Sample	N	$\Lambda^3 (10^{-23} \text{ m}^3)$	$E_a K_B^{-1} \text{ (K)}$	$K_{\text{bulk}} V_m \sqrt{N} K_B^{-1} \text{ (K)}$	$K_s (10^{-4} \text{ J/m}^2)$
Mn3	12	1.6 ± 0.2	841	6.5	1.2
Mn4	7	1.4 ± 0.1	2290	7.7	3.3
Mn6	5	6.1 ± 0.4	5563	37.7	2.9

almost the same correlation volume, the sample with bigger particles presents a bigger magnetic correlation volume. This is due to a bigger interparticle distance as the mean particle diameter increases, at fixed ϕ .

For short, we will name "magnetic cluster" the N particles in the magnetic correlation volume Λ^3 . It is important to stress that this correlation volume, evidenced in the magnetization measurements, do not show any additional electronic-density modulation at this length scale, otherwise it should be detected in the SAXS experiments ($0.15 \text{ nm}^{-1} < q_\Lambda < 0.23 \text{ nm}^{-1}$, where $q_\Lambda = 2\pi/\Lambda$, range accessible in our SAXS experiment).

The SW model hypotheses of noninteracting particles is not satisfied in the present case. Certainly, dipolar interactions are important enough for deviations from the expected behavior. Exchange bias (EB) in the same core-shell ferrite nanoparticles has already been investigated [18,19]. These nanoparticles consist of a well-ordered ferrimagnetic (FI) core surrounded by a disordered spin glass-like (SGL) surface layer and display uniaxial magnetic anisotropy. The exchange bias field sets at the internal interface FI-SGL of the nanoparticles. A comparison between frozen dispersions and disordered powder allows us to distinguish the influence of intra- and interparticle interactions on the exchange bias. Interparticle collective effects dominate in the powder while an intraparticle EB, eventually hindered by dipolar interactions at large volume fraction (demagnetizing role which reduces the exchange bias field value), is observed in frozen dispersions. In Ref. [19], the authors compare the exchange bias behavior for sample Mn3, based on nanoparticles of soft ferrite cores, with the exchange bias obtained for hard ferrite cores. The bias field is found to present a maximum, larger for harder ferrite core. It is obtained for a cooling field of the order of one half of the anisotropy field, which is much larger for the CoFe_2O_4 cores than for MnFe_2O_4 ones. In powders, particles are in contact leading to an interparticle exchange, which is not present in the dilute solutions. Exchange bias properties are only due to an intraparticle exchange between core and surface. The thermal dependence of the bias field is well described by a reduced exponential behavior with a characteristic freezing temperature of about $8K$.

Although a correlation between the magnetic moments of the nanoparticles has been found in all experiments performed, the SAXS curves (Fig. 1) are typical of dilute system, with no structure factor indications. This means that, in the q range investigated, the structure factor is $f_s = 1$, with no presence of any correlation peak or concentration effects. In the physical-chemical conditions of our samples the dispersion state is not that of a well-structured fluid, which would be required to present some kind of super-ferromagnetism [36].

Moreover, the superspin-glass behavior of a concentrated assembly of interacting maghemite nanoparticles has been recently studied [37], but those properties were obtained for volume fraction of particles of 35%. The superferromagnetism state would occur at larger volume fraction of NPs.

The existence of the interparticle interaction in the length-scale Λ imposes that the system respond to magnetic stimuli as composed by clusters of particles. This leads to a renormalized relaxation time and effective anisotropy K_{cluster} when compared to the single particle system. In fact, the energy barrier associated to the clusters increases by a factor \sqrt{N} with respect to a single particle case, according to the random anisotropy model [38], as shown in Eq. (10):

$$K_{\text{cluster}} \Lambda^3 = \left(K \frac{\phi}{\sqrt{N}} \right) \left(\frac{N V_m}{\phi} \right) = K V_m \sqrt{N}. \quad (10)$$

In order to determine the energy barrier and the relaxation time τ_0 of the samples, ac susceptibility measurements were performed as a function of temperature. The ac magnetic susceptibility has an *in phase* component χ' and an *out of phase* χ'' , related to dissipation losses [30] that peaks for $T = T_B$. As the blocking temperature is time dependent, the χ'' maximum position depends on the field frequency, moving toward higher temperatures as the field frequency increases. This behavior in our systems is shown in Fig. 3(a). From these data we obtain T_B at each frequency f . Equation 1 can be used to obtain τ_0 and E_a , fitting the expression $f^{-1} = \tau_0 \exp[E_a/(k_B T_B)]$ to these experimental data [see Fig. 3(b)]. The linear behavior observed in the experimental results of $\ln[1/(f \tau_0)] \times T_B^{-1}$ is characteristics of a thermal activated process. The obtained relaxation time $\tau_0 \sim 10^{-13}$ s does not correspond to a single particle relaxation time (which is in the range $\tau_0 = 10^{-9} \sim 10^{-12}$ s), in agreement with the previous interpretation of interacting particles [39,40].

The fit on Fig. 3(b) allows us to estimate the cluster's energy barrier E_a/k_B , which does not agree with the computed value $K_{\text{bulk}} V_m \sqrt{N}/k_B$ [Eq. (10)], as shown on Table II. This may be due to the fact that, besides the interactions between nanoparticles, confinement effects can change the value of the anisotropy constant of those particles. Typically, effects of the size reduction are taken into account assuming an effective value of the anisotropy constant, due to surface effects (K_s) [41] as shown on Eq. (11):

$$K_{\text{eff}} = K_{\text{bulk}} + \frac{6}{d} K_s. \quad (11)$$

Thus, by imposing $K_{\text{eff}}(V) \sqrt{N} = E_a$, one can estimate the surface effects on the nanoparticles effective anisotropy. In our case $K_s \sim 10^{-4} \text{ J/m}^2$, leading to $K_{\text{eff}} \sim 10^5 \text{ J/m}^3$ that corresponds to an increase of three orders of magnitude from

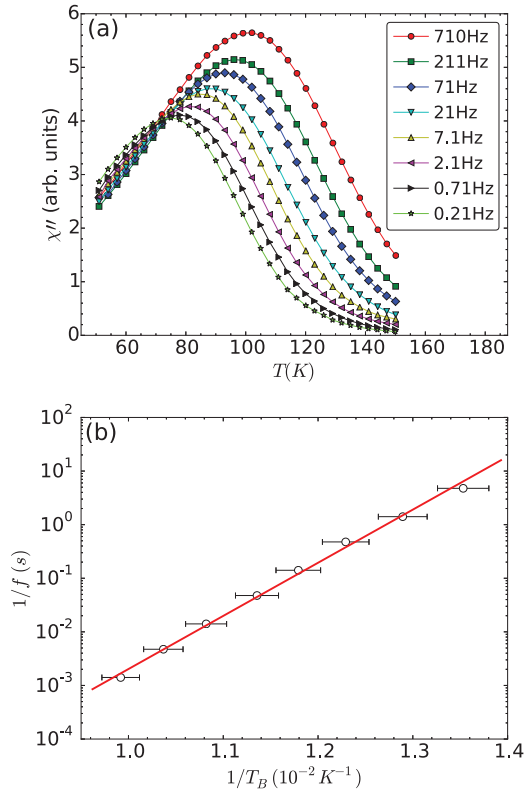


FIG. 3. (Color online) (a) ac susceptibility as a function of the temperature, for different field frequencies. (b) Inverse of the field frequency as a function of the blocking temperature.

the bulk value for $\text{MnFe}_2\text{O}_4@ \gamma\text{-Fe}_2\text{O}_3$. Calculated values of K_s for the three samples investigated are presented on Table II. The smallest value of K_s corresponds to the smallest nanoparticle.

We have shown that magnetic dipole interactions between nanoparticles are present in our system leading to magnetic clusters of interacting particles inside a correlation volume that can be seen as formed by “magnetic domains” where the particles momentum are correlated [1]. Magnetic measurements, as zero-field cooling-field cooling are sensible to those clusters instead of single particles. In this way, structural analysis as small angle x-rays scattering are of extreme importance to avoid erroneous interpretations of the data, bigger particles with narrower size distribution. Ac susceptibility measurements are in agreement with the existence of clusters by showing an extremely fast relaxation

process, with typical time τ_0 , that does not correspond to magnetic processes in a single particle [40].

V. SUMMARY

Magnetic fluids based on manganese ferrite nanoparticles were studied from the structural point of view through small angle x-rays scattering and from the magnetic point of view through zero-field cooling and field cooling and ac susceptibility measurements. The size distribution functions of three magnetic colloids were determined, as well as the mean diameter of the nanoparticles. The size distribution obtained from SAXS measurements follows, reasonably, a log-normal behavior, as usually assumed for those systems. From the ZFC-FC results the distribution of blocking temperatures were obtained and compared to those obtained with SAXS. The magnetic blocking temperature distribution was shown to be narrower than the structural one (from SAXS) due to the magnetic interactions between the nanoparticles that led to an averaging effect. The magnetic measurements indicate the existence of a magnetic correlation distance Λ in the colloidal medium that could be pictured as a magnetic cluster constituted by N interacting particles inside the correlation volume Λ^3 . These clusters are not characterized by a physical aggregation of particles, since the SAXS measurements do not reveal the existence of aggregates in a large number in the different samples analyzed. Besides the magnetic interaction between particles, confinement effects must be included to account for the experimental values of the magnetic energy barrier encountered. Due to the reduced size of the nanoparticles, surface effects play an important role in the determination of this parameter. Ac susceptibility measurements were crucial in the investigation of the interaction among nanoparticles since a very short relaxation time τ_0 was obtained from the magnetic measurements, which does not have any physical meaning for noninteracting particles. In that way, dipole interaction among nanoparticles must be taken into account for a correct interpretation of the magnetic and structural results.

ACKNOWLEDGMENTS

We thank CNPq (Conselho Nacional de Desenvolvimento Científico e Tecnológico), FAPESP (Fundação de Amparo à Pesquisa do Estado de São Paulo), CAPES (Coordenação de Aperfeiçoamento de Pessoal de Nível Superior), and INCT-FCx (Instituto Nacional de Ciência e Tecnologia de Fluidos Complexos) for financial support.

-
- [1] J. C. Denardin, A. L. Brandl, M. Knobel, P. Panissod, A. B. Pakhomov, H. Liu, and X. X. Zhang, *Phys. Rev. B* **65**, 064422 (2002).
- [2] S. Sankar, A. E. Berkowitz, and D. J. Smith, *Phys. Rev. B* **62**, 14273 (2000).
- [3] R. E. Rosensweig, *Ferrohydrodynamics* (Dover Publications, London, 2014).
- [4] C. Scherer and A. M. Figueiredo Neto, *Brazilian J. Phys.* **35**, 718 (2005).
- [5] B. A. Finlayson, *J. Fluid Mech.* **40**, 753 (1970).
- [6] K. Raj, B. Moskowitz, and R. Casciari, *J. Magn. Magn. Mat.* **149**, 174 (1995).
- [7] I. Sharifi, H. Shokrollahi, and S. Amiri, *J. Magn. Magn. Mat.* **324**, 903 (2012).
- [8] J. Durán, J. Arias, V. Gallardo, and A. Delgado, *J. Pharm. Sci.* **97**, 2948 (2008).
- [9] K. M. Krishnan, *IEEE Trans. Magn.* **46**, 2523 (2010).

- [10] R. Kitz, P. C. Fannin, and L. Trahms, *J. Magn. Magn. Mat.* **149**, 42 (1995).
- [11] M. B. Morales, M. H. Phan, S. Pal, N. A. Frey, and H. Srikanth, *J. Appl. Phys.* **105**, 07B511 (2009).
- [12] M. Hansen and S. Mørup, *J. Magn. Magn. Mat.* **203**, 214 (1999).
- [13] T. Wen, W. Liang, and K. M. Krishnan, *J. Appl. Phys.* **107**, 09B501 (2010).
- [14] M. Hanson, *J. Magn. Magn. Mat.* **96**, 105 (1991).
- [15] G. F. Goya and M. P. Morales, *Journal of Metastable and Nanocrystalline Materials* **20**, 673 (2004).
- [16] W. Nunes, W. Folly, J. Sinnecker, and M. Novak, *Phys. Rev. B* **70**, 014419 (2004).
- [17] P. Allia, G. Barrera, P. Tiberto, T. Nardi, Y. Leterrier, and M. Sangermano, *J. Appl. Phys.* **116**, 113903 (2014).
- [18] R. Cabreira-Gomes, F. G. Silva, R. Aquino, P. Bonville, F. Tourinho, R. Perzynski, and J. Depeyrot, *J. Magn. Magn. Mat.* **368**, 409 (2014).
- [19] F. G. Silva, R. Aquino, F. A. Tourinho, V. I. Stepanov, Y. L. Raikher, R. Perzynski, and J. Depeyrot, *J. Phys. D: Appl. Phys.* **46**, 285003 (2013).
- [20] S. Mørup, C. Frandsen, and M. F. Hansen, *Beilstein J. Nanotechnol.* **1**, 48 (2010).
- [21] P.-M. Déjardin, *J. Appl. Phys.* **110**, 113921 (2011).
- [22] G. T. Landi, *J. Appl. Phys.* **113**, 163908 (2013).
- [23] O. Glatter, *J. Appl. Crystallogr.* **10**, 415 (1977).
- [24] O. Glatter, *J. Appl. Crystallogr.* **13**, 7 (1980).
- [25] C. Kittel, *Rev. Modern Phys.* **21**, 541 (1949).
- [26] L. Néel, *Ann. Géophys.* **5**, 99 (1949).
- [27] E. Wohlfarth, *Phys. Lett. A* **70**, 489 (1979).
- [28] M. Suzuki, S. I. Fullem, and I. S. Suzuki, *J. Magn. Magn. Mat.* **322**, 3178 (2010).
- [29] R. Chantrell, M. El-Hilo, and K. O'Grady, *IEEE Trans. Magn.* **27**, 3570 (1991).
- [30] M. Fldeáki, G. Higelin, L. Kszegi, B. Schwendemann, and F. Walz, *J. Magn. Magn. Mat.* **46**, 350 (1985).
- [31] F. A. Tourinho, R. Franck, and R. Massart, *J. Materials Sci.* **25**, 3249 (1990).
- [32] J. A. Gomes, M. H. Sousa, F. A. Tourinho, R. Aquino, G. J. da Silva, J. Depeyrot, E. Dubois, and R. Perzynski, *J. Phys. Chem. C* **112**, 6220 (2008).
- [33] R. Aquino, F. A. Tourinho, R. Itri, and J. Depeyrot, *J. Magn. Magn. Mat.* **252**, 23 (2002).
- [34] E. C. Stoner and E. P. Wohlfarth, *Philos. Trans. R. Soc. A: Math. Phys. Eng. Sci.* **240**, 599 (1948).
- [35] S. Sankar, A. Berkowitz, D. Dender, J. Borchers, R. Erwin, S. Kline, and D. J. Smith, *J. Magn. Magn. Mat.* **221**, 1 (2000).
- [36] S. Bedanta and W. Kleemann, *J. Phys. D: Appl. Phys.* **42**, 013001 (2009).
- [37] D. Parker, V. Dupuis, F. Ladieu, J.-P. Bouchaud, E. Dubois, R. Perzynski, and E. Vincent, *Phys. Rev. B* **77**, 104428 (2008).
- [38] R. Alben, J. J. Becker, and M. C. Chi, *J. Appl. Phys.* **49**, 1653 (1978).
- [39] X. X. Zhang, J. M. Hernandez, J. Tejada, and R. F. Ziolo, *Phys. Rev. B* **54**, 4101 (1996).
- [40] X. X. Zhang, G. Gu, H. Huang, S. Yang, and Y. Du, *J. Phys.: Condensed Matter* **13**, 3913 (2001).
- [41] F. Bødker, S. Mørup, and S. Linderroth, *Phys. Rev. Lett.* **72**, 282 (1994).